AIAA JOURNAL
Vol. 31, No. 12, December 1993

Numerical Simulation of Confined Transonic Normal Shock Wave/Turbulent Boundary-Layer Interactions

Edwin Blosch* and Bruce F. Carroll†
University of Florida, Gainesville, Florida 32611
and
Martin J. Morris‡
McDonnell Douglas Aerospace, St. Louis, Missouri 63166

A numerical simulation and experimental investigation of a steady, two-dimensional, Mach 1.48 normal shock wave/turbulent boundary-layer interaction (NSTBLI) in a diffuser configuration have been conducted. This paper reports the results of the numerical simulation. Compared to previous investigations, the flow problem is distinguished by the relatively large ratio of boundary-layer thickness to duct height (0.1) at the beginning of the NSTBLI, and the adverse pressure gradient imposed on the recovering boundary layer by duct divergence. High levels of initial blockage change the displacement thickness variation through the NSTBLI and increase the incipient separation Mach number, whereas the adverse downstream pressure gradient alters the boundary-layer recovery following the shock. The motivation for this research is a better understanding of the role of the various parameters influencing the global features of NSTBLIs. Computations of wall static pressure, displacement thickness, and shape factor distributions and contours of the streamwise component of velocity and Reynolds stress are compared with experiment.

Nomenclature

C_f	=coefficient of skin friction
H	=boundary-layer shape factor
h	=diffuser height at normal shock location
h_{bif}	=distance of bifurcation point from top wall
M	=Mach number
Re	=Reynolds number
y^+	=Reynolds number based on wall variables
δ	=boundary-layer thickness
δ^*	=displacement thickness
θ	=momentum thickness
μ_t	=turbulent viscosity
$<>$	=ensemble-averaged quantity
Subscripts	
i	=incompressible quantity
u	=undisturbed location upstream of shock
x	=streamwise coordinate
∞	=freestream value
Superscripts	
$'$	=fluctuation of time-averaged quantity
$''$	=fluctuation of mass-averaged quantity

Introduction

SHOCK-INDUCED flow separation in supersonic inlet and wind-tunnel diffusers leads to poor pressure recovery characteristics, dramatic increases in turbulence intensity, and downstream flow nonuniformity. For inlet design there is a strong motivation to understand the basic physics of shock wave/boundary-layer interactions (SBLIs), in order to devise successful means of controlling the interaction, for example, by suction.[1] The review papers of Délery[2] and Green[3] discuss approaches toward boundary-layer control in SBLIs, describe the structure of the interaction region in detail, and provide a bibliography for SBLI research over the past 40 years. Much of the previous research on normal shock wave/turbulent boundary-layer interactions (NSTBLIs) has focused on two-dimensional unconfined interactions on flat, adiabatic, smooth, and impermeable plates (or walls) in constant-area ducts, in order to identify the basic governing parameters and understand the boundary-layer development through the shock wave. In real situations, however, the flow blockage (also called confinement) is often substantial; the turbulent boundary layer approaching the normal shock wave is relatively thick compared to the diffuser height ($\delta_u/h \geq 0.1$). Few investigations have considered NSTBLIs under these conditions.[4–8] The goal of the present research is to investigate numerically the combined effects of a significant level of blockage ($\delta_u/h \simeq 0.1$) and a mild adverse pressure gradient downstream of the NSTBLI, under common flow conditions.[2,6,9–12] To this end, a numerical simulation of a steady, two-dimensional, Mach 1.48 NSTBLI in a diffuser configuration has been conducted, and the results compared with the experimental data of Morris et al.[13] and the findings of other researchers. This research has also provided a starting point for a parametric study of local suction on the NSTBLI.

Far upstream of the shock wave, the turbulent boundary layer developing on an adiabatic flat plate or wall under a zero streamwise pressure gradient has a law of the wall/wake structure. At a distance that is $O(\delta_u)$ upstream of the shock wave, called the upstream influence length, compression waves are created by thickening of the subsonic stream tube, in response to the high downstream pressure imposed by the normal shock. These waves coalesce with the normal shock, bending and weakening it so that a continuous pressure rise occurs along the sonic boundary of the subsonic stream tube. If the adverse pressure gradient is steep enough, separation occurs, usually upstream of the normal shock wave. This happens for $1.3 < M < 1.4$, although flow confinement can delay separation up to Mach numbers as high as 1.6 (Ref. 14). In the context of this research, confinement refers to the constraining effect of the far field (walls) on the velocity of the inviscid core flow, which modifies the natural development of the boundary layer through the NSTBLI. Typically, the ratio δ_u/h is used as a flow confinement parameter. The flow confinement concept applies to oblique SBLIs also, but is fundamentally different since the flow behind the shock wave is still hyperbolic, so the far field

Received July 17, 1992; revision received March 8, 1993; accepted for publication March 8, 1993.

*Graduate Student, Department of Aerospace Engineering. Member AIAA.
†Assistant Professor, Department of Aerospace Engineering. Member AIAA.
‡Scientist. Member AIAA.

has a limited influence in the interaction region. Shock-induced separation coincides with a coupling of the inner viscous-important layer with the outer irrotational flow,[15] leading to the typical bifurcated shock foot described by Seddon[9] and the "free interaction" effect described by Green,[3] so named because the upstream thickening of the subsonic part of the boundary layer and compression in the supersonic part of the boundary layer reinforce one another. Consequently, the flow features up to the separation point, for a given Mach number and wall shape, depend only on the properties of the incoming boundary layer, that is, $Re_{\delta,u}$, H_i, and the heat flux condition at the wall.[2] Following the bifurcated shock, a supersonic velocity overshoot that is $O(10\delta_u)$ long can occur.[6,9,12] Its cause is streamline convergence brought about by the curvature of the shock wave within the supersonic part of the boundary layer,[7] the growth of δ^* through the interaction,[6] and the constraints of the far field on the direction of the inviscid core flow (flow confinement).[7] The jumps in δ^* and θ across an NSTBLI increase with Mach number and H_i and decreasing δ_u/h, but are insensitive to $Re_{\delta,u}$. With large confinement effects, the entire post shock flow reaccelerates and multiple normal shocks (shock trains),[7,16–18] or series of oblique shocks,[14,16,18] are observed.

Formulation

The governing equations for which a numerical solution has been found are the mass-averaged two-dimensional Navier-Stokes equations in conservation law form. A steady-state solution to the flow problem was obtained using the time-marching technique, with MacCormack's explicit, unsplit, predictor-corrector scheme.[19] The turbulent viscosity μ_t is computed by the modified Prandtl-van Driest mixing length formulation developed by Baldwin and Lomax.[20] From the separation point to a user-specified distance downstream of reattachment, the second peak in the outer length scale function, if present, was selected. Visbal and Knight[21] obtained larger values of μ_t and consequently better agreement with experimental data by using this modification. Their suggestion of using the local shear stress instead of the wall shear stress in the reattachment region was employed. Otherwise, μ_t from the inner layer formulation is underestimated, which delays reattachment. The original model constants[20] were used in the present implementation, which was first coded by Kumar[22] and has since been extensively modified by Carroll.[23] The Baldwin-Lomax model is computationally inexpensive, easy to understand, and has been used for many compressible aerodynamics problems with small separated regions; used carefully, it is adequate for quantitative analysis. Two-equation turbulence models are generally better than algebraic models for SBLI simulations, but they still do not accurately predict, without adjusting the parameters of the model, all the mean flow features of interest.[5,15,24]

The physical domain chosen for numerical simulation begins in the approach section of the diffuser configuration described in detail by Morris et al.[13] and shown in Fig. 1. In the experiment, a symmetric, two-dimensional nozzle generates a uniform $M_\infty = 1.5$ flow in a high-aspect-ratio duct (2.9) whose bottom wall diverges slightly (0.19 deg) to account for boundary-layer growth. The sidewall boundary layers are diverted through slots 270 mm upstream of the normal shock, which is positioned at the leading edge of a splitter plate ($x = 0$ mm) by adjusting the downstream static pressure using a flap. The splitter plate diverts the bottom wall boundary layer through an upstream-facing slot, so that the top wall boundary layer is responsible for the majority of the blockage through the interaction region. The NSTBLI takes place on the solid top wall of the duct, beginning at about $x = -31$ mm, and the duct begins to diverge at $x = 31.7$ mm, imposing a mild adverse pressure gradient on the reattaching boundary layer. Morris et al.[13] observed that the top and bottom wall boundary layers merged at $x = 130$ mm, but cross-section contours of velocity components indicated that a high degree of two-dimensionality was achieved up to $x = 250$ mm. Following the work of Shea, a blockage number Bk is defined as the fraction of the flow area occupied by the boundary-layer displacement thickness. For our case, $Bk = 0.02$ just upstream of the interaction, with 10% of the total blockage coming from the side wall boundary layers. Further downstream at $x = 80$ mm, $Bk = 0.19$ with the side wall boundary layer contributing only 15% of the total blockage. The present computational domain includes the top and bottom walls and thus captures the majority of the blockage effect. In contrast, Shea's computation[25] of Seddon's[9] experimental interaction was limited to one wall of the wind tunnel with the upper edge of the computational domain modeled as a freestream boundary. Although the blockage number was $Bk = 0.023$, which is similar to the current case, the side wall boundary layers contributed two-thirds of the total blockage and special freestream boundary conditions were required to accurately model the flow confinement effect.

The domain of the current simulation was from -70 mm $\leq x \leq 300$ mm. A 129×77 grid was used, with approximately 25 points within the boundary layer in the interaction region. The first grid point off the wall occurred at $y^+ \leq 10$, using a first-order estimate for the wall shear stress. In the streamwise direction, the grid points are spaced at approximately 1-mm intervals, smoothly increasing to 6 mm at the exit plane, where streamwise gradients are small. The normal shock was captured over three grid lines. A grid-refinement study indicated adequate grid resolution. The bottom wall slot was modeled by extending the computational domain into the slot and applying outflow boundary conditions well downstream of the splitter plate tip. No-slip conditions for the u and v components of velocity were applied on the solid boundaries, with the density and pressure determined by first-order extrapolation. Inflow conditions were taken from the experimental velocity profile data[13] and known values for total pressure and temperature. Static pressure is specified at the outflow boundary because the

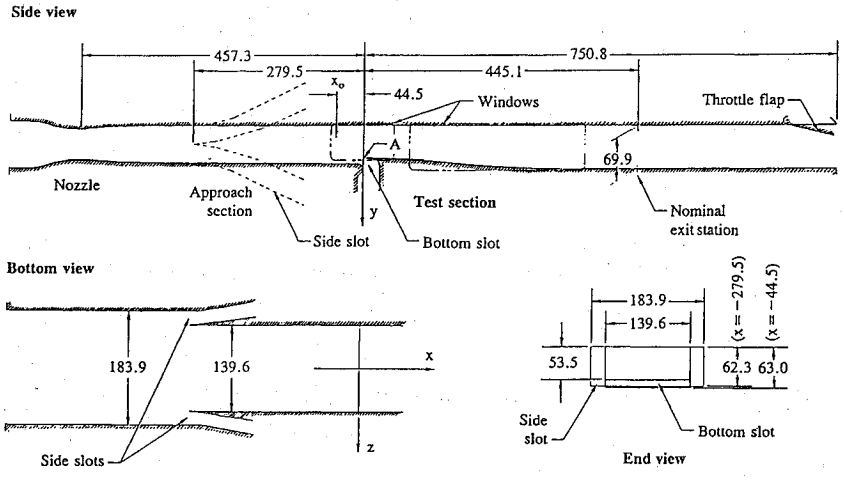

Note: All dimensions are in mm.

Fig. 1 Experimental setup for confined $M_\infty = 1.48$ NSTBLI study. Taken from Morris et al.[13]

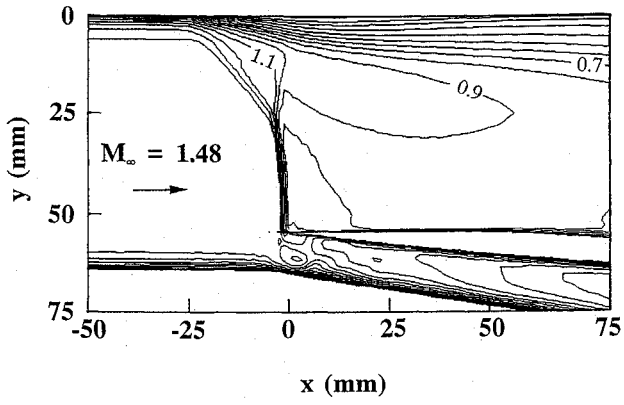

Fig. 2 Computed Mach contours, $\Delta M = 0.1$, showing the bifurcated normal shock and modeled bottom wall slot.

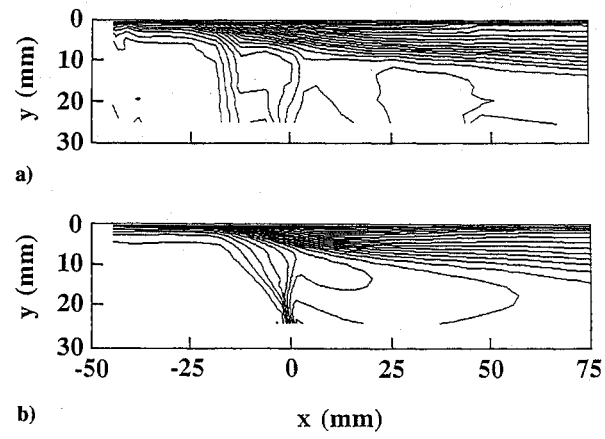

Fig. 3 Contour of u/a^*: a) experiment and b) computed. To facilitate comparison, the computed solution is shown only in the region where LDV data were collected; the computational domain extends beyond the area shown.

flow is subsonic, and the other dependent variables at the exit plane are determined using a nonreflecting reference plane characteristics scheme.[23,26] An initial value plane was constructed using one-dimensional normal shock and isentropic flow with area change relationships, with the shock positioned at the holder, but a separation bubble formed on the top wall at the normal shock during the initial transient stage of the computation. This choked the flow in the constant-area section ($0 \le x \le 31.7$ mm), forcing the shock to move upstream, off of the holder. Shock-induced separation then followed on the bottom wall, at the entrance to the bleed slot, choking it too, and causing spillage around the leading edge of the splitter plate. This effectively prevented the normal shock from relaxing back to the shock holder. An alternate, successful initial guess was created by positioning the normal shock in the diverging section of the duct. Trial and error was then necessary to determine the exit pressure that stabilized the normal shock at the tip of the splitter plate.

Discussion of Results

A converged solution was obtained in 4×10^5 time steps, which was approximately 0.1 s in real time. The exit pressure, at $x = 300$ mm, was overpredicted by 4%, which may be due in part to sidewall boundary-layer growth accelerating the core flow in the experiment. A small separation on the bottom wall (opposite the wall of interest) in the diverging section of the duct, observed in the experiment but not captured in the computation, may have also contributed to this effect. Figure 2 shows the computed Mach contours for -50 mm $< x < 75$ mm and also indicates the modeled geometry of the shock holder. The top wall static pressure begins to rise at $x = -31$ mm; this is called the undisturbed location (subscript u). Thus, the upstream influence length is 31 mm, smaller than the experimental value of 45 mm. This disagreement stems from the selection of the second peak in the outer length scale function of the Baldwin-Lomax model, in the region just downstream of the separation point where the turbulence has not yet responded to the mean flow gradients.[21] At the undisturbed location, the boundary-layer shape factor determined from the LDV data was $H_{i,u} = 1.45$, whereas in the simulation $H_{i,u} = 1.35$. In the computation and experiment, the boundary-layer thickness was $\delta = 6.0$ mm, which yields $Re_{\delta,u} = 2.3 \times 10^5$, and the incompressible displacement thickness was $\delta_i^* = 0.7$ mm. The incoming Mach number was 1.48, both experimentally and computationally.

In Fig. 2, the normal shock bends forward slightly as it approaches the top wall and bifurcates. These features were also observed experimentally using high-speed schlieren pictures, although the bifurcation point was farther from the top wall in the experiment. A high-speed velocity overshoot extending far downstream of the bifurcation point occurs, but it is not supersonic. Like Seddon's $M_\infty = 1.48$ NSTBLI,[9] the thickness of this overshoot decreases downstream, in contrast to the observations of Om et al.[6] and Carroll and Dutton,[7,16] both conducted at higher confinement levels. The thickness of the supersonic overshoot increases with Mach number[6] and blockage δ_u/h (Ref. 5) and decreasing unit Re. (Refs. 6 and 16) The confinement ratio for Seddon's $M_\infty = 1.48$ NSTBLI was the same as in the present simulation, $\delta_u/h = 0.1$, but $Re_{\delta,u}$ was an order of magnitude smaller. Thus, $Re_{\delta,u}$ helps determine whether or not velocity overshoots in confined NSTBLIs are supersonic.

The bifurcation point is $h_{\text{bif}} = 3.9\delta_u$ from the top wall in the experiment, whereas the simulation gives $h_{\text{bif}} = 3\delta_u$ (see Fig. 2). Because the upstream interaction length is smaller in the simulation, the leading leg of the shock foot originates further downstream and intersects the normal shock wave nearer the top wall. The results of other researchers also indicate the importance of H_i in determining the upstream influence length and h_{bif}, notably those of Délery,[2] who obtained a correlation valid for weak interactions that relates $H_{i,u}$, δ_u, and the upstream influence length. Vidal et al.[11] observed a bifurcation height scaling with Re_x, and reported $h_{\text{bif}} = 4.25\delta_u$ for a $M_\infty = 51.4$ separated NSTBLI at $Re_x = 9 \times 10^6$, decreasing to $h_{\text{bif}} = 2.5\delta_u$ as Re_x increased to 36×10^6. The Reynolds number based on an undisturbed boundary-layer thickness was 5×10^5 in both cases since the location of the shock generator in their experiments was positioned to keep δ_u fixed. This suggests that $H_{i,u}$ may have increased with Re_x, leading to the observed decrease in h_{bif}. Vidal et al.[11] also noted a large decrease in the upstream influence length as Re_x increased, which is consistent with an increase in $H_{i,u}$. Both Om et al.[6] and

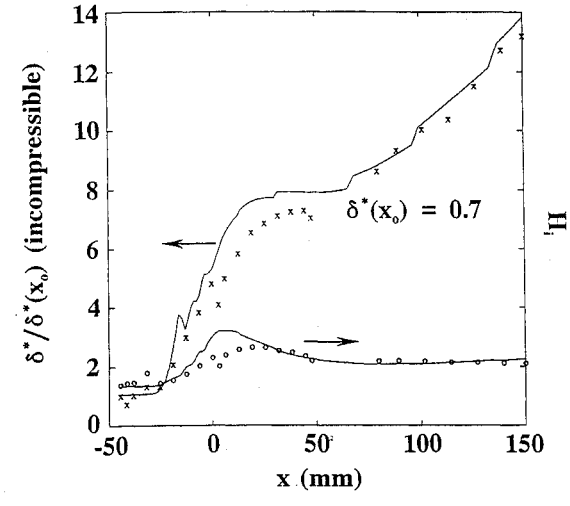

Fig. 4 Incompressible boundary-layer displacement thickness and shape factor. The upper curve is nondimensionalized displacement thickness, where x denotes experimental values. Experimental values for H_i are denoted by the symbol o.

Seddon[9] report $h_{bif} \simeq 5\delta_u$. In each of the experiments, $Re_{\delta,u}$ was an order of magnitude less than in the present computation and Vidal et al.,[11] which suggests that h_{bif} decreases with increasing $Re_{\delta,u}$. Neither Seddon[9] nor Om et al.[6] report $H_{i,u}$, but the boundary layers entering the interaction were in each case developed under a zero pressure gradient along flat surfaces, so a correlation between $Re_{\delta,u}$ and H_i is expected,[2] namely that $Re_{\delta,u}$ increasing implies H_i decreasing. From the results just discussed, it appears that h_{bif} increases when the velocity profile entering the interaction is less full (low $Re_{\delta,u}$ or high $H_{i,u}$). The quantity h_{bif} is significant because it is the distance from the wall to the vortex sheet that originates at the bifurcation point and extends far downstream[6,9] of the interaction.

Figure 3 compares the computed and measured u component of velocity contours for the top half of the duct, which is where LDV data were collected. The boundary layer appears to grow at the correct rate downstream of the interaction, but the shock wave is significantly sharper than in the experimental data. This is caused primarily by the contour plotting package fitting curves between the coarse streamwise LDV grid. Figure 4 shows that the predicted displacement thickness growth does indeed agree well with experimental data, particularly in the region following reattachment. This occurs in spite of the underprediction of the upstream influence length and suggests that these parameters are not excessively sensitive to the turbulence model. The overprediction of H_i and δ^* within the interaction region may be related to the absence of negative mean u components of velocity in the LDV data. LDV measurements were obtained up to 0.25 mm from the wall. Although the majority of instantaneous samples indicated reversed flow and surface oil-flow techniques clearly showed separation beginning at $x = -10$ mm, time-averaged u values were positive. Kooi,[12] Om et al.,[6] and Vidal et al.[11] used pitot and static probe measurements to construct velocity profiles, but were also unable to detect reversed flow based on those data alone. From the LDV data, Morris et al.[13] constructed probability contours in the region where data were collected, reflecting the fraction of velocity samples that indicated reversed flow. If these contours are extrapolated to the wall, the present computed separation bubble, which lies in -13 mm $\leq x \leq 50$ mm, agrees best with the experimental data contour that bounds the region of probability $P \geq 0.1$. The actual reattachment location was not discernible from the surface oil-flow visualization.

The computed top wall static pressure and skin friction coefficient variation are shown in Fig. 5. The computed pressure rise begins farther downstream and is steeper than in the experiment, which is attributed in part to the differences in $H_{i,u}$, which was previously discussed. Visbal and Knight[21] and Mateer et al.[10] have observed the same discrepancy in their simulations that employed various algebraic turbulence models[5,21]; it is attributed to the overprediction of μ_t in the region near the separation point where the turbulence is not in equilibrium. The wall pressure further downstream increases at the correct rate, although it is higher than measured. The shape of the C_f distribution is similar to that computed by Mateer et al.,[10] who used two relaxation corrections in addition to a baseline mixing length model. Each model underpredicted the skin friction downstream of reattachment; the baseline model performed slightly better than the models with relaxation in this respect. They also saw a decrease in the slope of the C_f curve through reattachment, as in Fig. 5, increasing again further downstream. In the present computation, however, C_f begins to return to zero about 25 mm downstream of reattachment, instead of continuing to increase. This is due to the duct divergence in the present flow problem.

Figure 6 shows nondimensionalized top wall velocity profiles at several streamwise locations. At $x = -19$ mm, the computed profile is noticeably fuller than measured, reflecting the discrepancy in upstream influence length. The velocity overshoot for $x = 0$, 6, and 13 mm profiles is captured in the simulation, as is the inflection point in the velocity profiles $x = 25$, 38, 45, and 79 mm, around the reattachment location. The near wall "filling out" of the velocity profile downstream of reattachment is underpredicted, as was also observed by Visbal and Knight[21] and Mateer et al.[10] In the core flow region downstream of the interaction, the velocity is under-

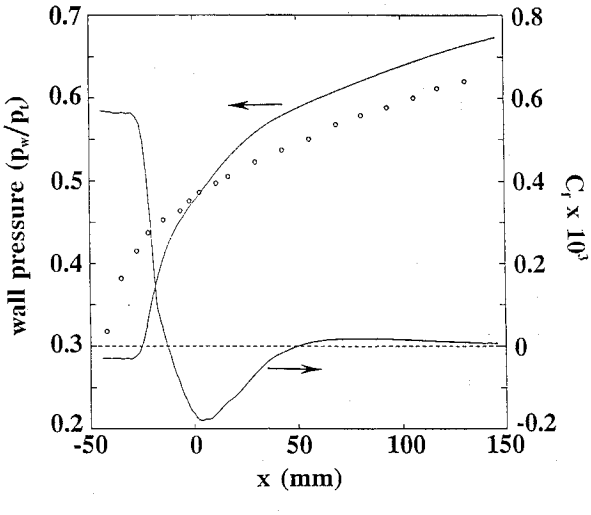

Fig. 5 Computed top wall static pressure and skin friction coefficient distributions. Experimental wall pressure data are denoted by the symbol o. The total pressure $p_t = 240$ kPa.

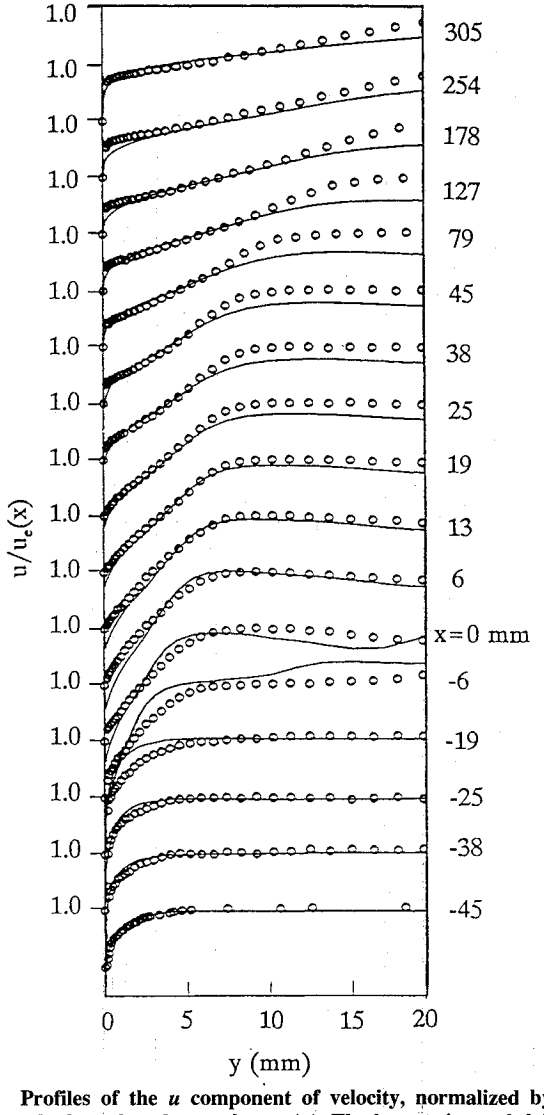

Fig. 6 Profiles of the u component of velocity, normalized by the value at the boundary-layer edge, $u_e(x)$. The lowest tic mark labeled 1.0 belongs to the profile at $x = -45$ mm. Profiles for other x locations are shifted successively upward, each by 0.5.

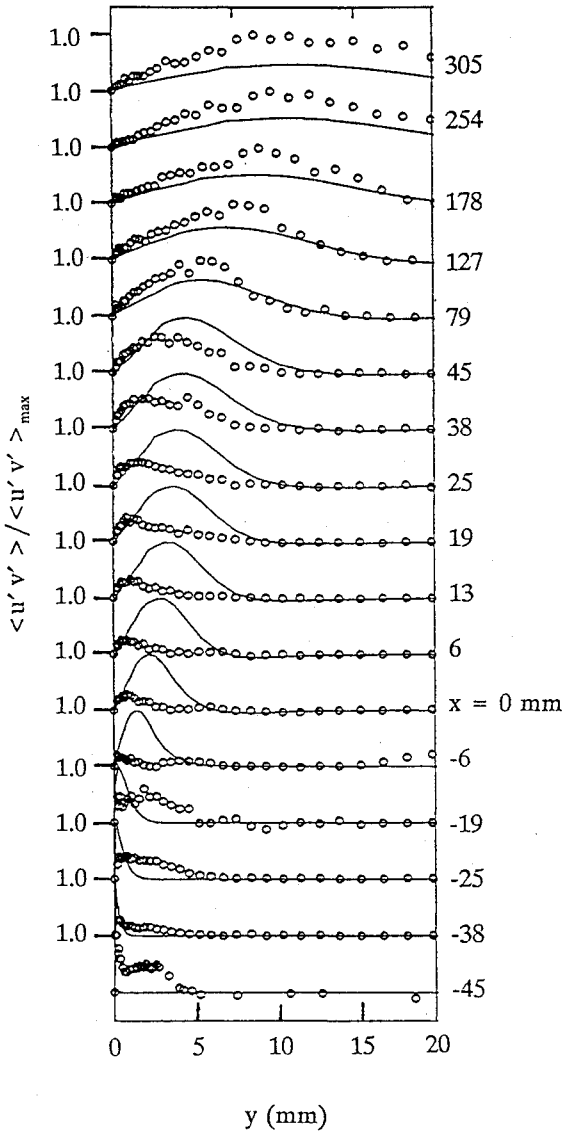

Fig. 7 Profiles of kinematic Reynolds shear stress $<u'v'>$, normalized by the maximum value in the experimental or computed profile, $<u'v'>_{max}$. The lowest tic mark labeled 1.0 belongs to the profile at $x=-45$ mm. Profiles for other x locations are shifted successively upward, each by 1.0.

predicted. This is due, in part, to side wall boundary-layer growth. However, as was stated here, the side wall contributes only a small fraction of the total blockage.

From the computed turbulent viscosities one can estimate the kinematic Reynolds stress $<u'v'>$ as follows:

$$\mu_t\left(\frac{\partial u}{\partial y}+\frac{\partial v}{\partial x}\right) = \langle \rho u''v''\rangle \simeq \langle \bar{\rho}u'v'\rangle$$

where the last step requires Morkovin's hypothesis for the neglect of $<\rho'(\ )>$ terms compared with $<\rho(\ )>$ terms for the low Mach number range. Examination of computed kinematic Reynolds shear stresses, illustrated in Fig. 7, shows that the Baldwin-Lomax model overpredicts by a factor of 2 the peak value of $<u'v'>$ for -19 mm $\leq x \leq 25$ mm, and that the peak in $<u'v'>$ begins to move away from the top wall at $x=-6$ mm, instead of at $x=13$ mm as in the experiment. The peak is farther from the wall than measured until $x=79$ mm, which is 25 mm downstream of the reattachment location. Farther downstream, $<u'v'>$ based on the values of μ_t computed using the Baldwin-Lomax model agree well with the experimental data; both the computed and measured peaks in $<u'v'>$ continue to move farther from the wall and diminish in magnitude. No effort was made to improve the agreement by adjusting the model constants or arbitrarily limiting the increase in the turbulence viscosity.

Recommendations

The simulation using the Baldwin-Lomax model adequately reflected certain important features of this complex flowfield, such as the bifurcated shock pattern and downstream recovery of the boundary layer. Flow confinement effects are moderate in this flowfield, in that a velocity overshoot similar in shape to the one observed by Seddon[9] is predicted, but reacceleration of the core flow as in Carroll and Dutton[7] and Om et al.[6] is not seen. The mild adverse pressure gradient in the region of recovery does not prevent reattachment, but does result in a small, nearly constant value for the skin friction in the region where the boundary-layer velocity profile usually recovers in single NSTBLIs conducted in constant-area ducts.[2,10] The computation was able to predict displacement thickness and shape factor downstream of the interaction, indicating that useful design information can be obtained with the algebraic turbulence model. Following the approach of Mateer et al.,[10] it would be instructive to add a relaxation parameter to the Baldwin-Lomax formulation and compare the results of the two simulations. A two-equation turbulence model would then be a reasonable next step in order to assess the importance of transport for the boundary-layer recovery in the presence of the adverse pressure gradient. The present work has also provided a starting point for an investigation of the effects of suction on this same NSTBLI.[27]

Acknowledgments

This research was conducted with partial support from the McDonnell Douglas Independent Research and Development program, the DOE Computational Science Graduate Fellowship administered by Oak Ridge Associated Universities, and the National Center for Supercomputing Applications, who provided computational resources.

References

[1]Waltrup, P. J., "Liquid Fueled Supersonic Combustion Ramjets: A Research Perspective of the Past, Present, and Future," AIAA Paper 86-0158, Jan. 1986.

[2]Délery, J., "Shock-Wave/Turbulent Boundary-Layer Interaction and Its Control," *Progress in Aerospace Sciences,* Vol. 22, Pergamon, New York, 1985, pp. 209–280.

[3]Green, J. E., "Interactions Between Shock Waves and Turbulent Boundary Layers," *Progress in Aeronatical Sciences,* Vol. 11, Pergamon, New York, 1970, pp. 235–340.

[4]Sajben, M., Morris, M. J., Bogar, T. J., and Kroutil, J. C., "Confined Normal-Shock/Turbulent-Boundary-Layer Interaction Followed by an Adverse Pressure Gradient," AIAA Paper 89-0354, Jan. 1989.

[5]Mateer, G. G., and Viegas, J. R., "Effect of Mach and Reynolds Numbers on a Normal Shock-Wave/Turbulent Boundary-Layer Interaction," AIAA Paper 79-1502, July 1979.

[6]Om, D., Childs, M. E., and Viegas, J. R., "An Experimental Investigation and a Numerical Prediction of a Transonic Normal Shock Wave/Turbulent Boundary Layer Interaction," *AIAA Journal,* Vol. 20, No. 5, 1985, pp. 707–714.

[7]Carroll, B. F., and Dutton, J. C., "Multiple Normal Shock Wave/Turbulent Boundary Layer Interactions," *Journal of Propulsion and Power,* Vol. 8, No. 2, 1992, pp. 441–448.

[8]Carroll, B. F., and Dutton, J. C., "Turbulence Phenomena in a Multiple Normal Shock Wave/Turbulent Boundary-Layer Interaction," *AIAA Journal,* Vol. 30, No. 1, 1992, pp. 43–48.

[9]Seddon, J., "The Flow Produced by Interaction of a Turbulent Boundary Layer with a Normal Shock Wave of Strength Sufficient to Cause Separation," Aeronautical Research Council Reports and Memoranda No. 3502, London, March 1960.

[10]Mateer, G. G., Brosh, A., and Viegas, J. R., "A Normal Shock-Wave Turbulent Boundary-Layer Interaction at Transonic Speeds," AIAA Paper 76-161, Jan. 1976.

[11]Vidal, R. J., Wittliff, C. E., Catlin, P. A., and Sheen, B. H., "Reynolds Number Effects on the Shock Wave–Turbulent Boundary Layer Interaction at Transonic Speeds," AIAA Paper 73-661, July 1973.

[12]Kooi, J. W., "Experiment on Transonic Shock-Wave Boundary Layer Interaction," AGARD Conference Proceedings No. 168, *Flow Separation,*

NATO, London, May 1975.

[13]Morris, M. J., Sajben, M., and Kroutil, J. C., "Experimental Investigation of Normal-Shock/Turbulent-Boundary-Layer Interactions with and Without Mass Removal," *AIAA Journal,* Vol. 30, No. 2, 1992, pp. 359–366.

[14]Carroll, B. F., and Dutton, J. C., "Characteristics of Multiple Shock Wave/Turbulent Boundary-Layer Interactions in Rectangular Ducts," *Journal of Propulsion and Power,* Vol. 6, No. 2, 1990, pp. 186–193.

[15]Adamson, T. C., and Messiter, A. F., "Analysis of Two-Dimensional Interactions Between Shock Waves and Boundary Layer," *Annual Review of Fluid Mechanics,* Vol. 12, 1980, pp. 103–138.

[16]Carroll, B. F., and Dutton, J. C., "Computation of Multiple Normal Shock Wave/Turbulent Boundary Layer Interactions," AIAA Paper 90-2133, July 1990.

[17]Merkli, P. E., "Pressure Recovery in Rectangular Constant Area Supersonic Diffusers," *AIAA Journal,* Vol. 14, No. 2, 1976, pp. 168–172.

[18]Lustwerk, F., "The Influence of Boundary Layer on the 'Normal' Shock Configuration," Meteor Rept. No. 61, Massachusetts Inst. of Technology Guided Missiles Program, Cambridge, MA, Sept. 1950.

[19]MacCormack, R. W., "The Effect of Viscosity in Hypervelocity Impact Cratering," AIAA Paper 69-354, Jan. 1969.

[20]Baldwin, B. S., and Lomax, H., "Thin Layer Approximation and Algebraic Model for Separated Turbulent Flows," AIAA Paper 78-257, Jan. 1978.

[21]Visbal, M., and Knight, D., "The Baldwin-Lomax Turbulence Model for Two-Dimensional Shock-Wave/Boundary-Layer Interactions," *AIAA Journal,* Vol. 22, No. 7, 1984, pp. 921–928.

[22]Kumar, A., "User's Guide for NASCRIN—A Vectorized Code for Calculating Two-Dimensional Supersonic Internal Flow Fields," NASA TM 85708, Feb. 1984.

[23]Carroll, B., "A Numerical and Experimental Investigation of Multiple Shock Wave/Turbulent Boundary Layer Interactions in a Rectangular Duct," Ph.D. Thesis, Dept. of Mechanical and Industrial Engineering, Univ. of Illinois at Urbana-Champaign, Urbana, IL, 1988.

[24]Viegas, J. R., and Horstmann, C. C., "Comparison of Multiequation Turbulence Models for Several Shock Boundary-Layer Interaction Flows," *AIAA Journal,* Vol. 17, No. 8, 1979, pp. 811–820.

[25]Shea, J. R., "A Numerical Study of Transonic Normal Shock-Turbulent Boundary Layer Interactions," AIAA Paper 78-1170, July 1978.

[26]Cline, M. C., "VNAP: A Computer Program for Computation of Two-Dimensional, Time-Dependent, Compressible, Viscous, Internal Flow," Rept. No. LA-7326, Los Alamos National Lab., Los Alamos, NM, Nov. 1978.

[27]Overholt, M., "Suction Boundary Conditions for the Analysis of Normal Shock/Turbulent Boundary Layer Interactions," M.S. Thesis, Dept. of Aerospace Engineering, Mechanics and Engineering Science, Univ. of Florida, Gainesville, FL, 1992.